Applied Catalysis B: Environmental 132–133 (2013) 487–492

Contents lists available at SciVerse ScienceDirect

Applied Catalysis B: Environmental

journal homepage: www.elsevier.com/locate/apcatb

Efficient persistent photocatalytic decomposition of nitrogen monoxide over a fluorescence-assisted $CaAl_2O_4$:(Eu, Nd)/(Ta, N)-codoped TiO_2/Fe_2O_3

Huihui Li[a,b,*], Shu Yin[a,**], Yuhua Wang[b], Tsugio Sato[a]

[a] Institute of Multidisciplinary Research for Advanced Materials, Tohoku University, 2-1-1, Katahira, Aoba-ku, Sendai 980-8577, Japan
[b] School of Physical Science and Technology, Lanzhou University, PR China

ARTICLE INFO

Article history:
Received 8 August 2012
Received in revised form
24 November 2012
Accepted 2 December 2012
Available online 26 December 2012

Keywords:
Compensated codoping
Loading
Coupling
Persistent fluorescence assisted
Visible-light
Photocatalyst

ABSTRACT

An effective promoting approach was described to modify the photoelectrochemical properties of rutile TiO_2 by codoping with the nonmetal N and transition metal Ta ions, followed by loading with Fe_2O_3. Here, the charge compensated and coupled semiconductor systems were constructed, and their visible-light and persistent fluorescence assisted photocatalytic activities for NO destruction and CH_3CHO removal were evaluated. The results demonstrated that both the charge compensation of TiO_2 by co-doping with N^{3-} and Ta^{5+} and loading with a proper amount of Fe_2O_3 facilitated the enhancement of both the visible-light and persistent fluorescence induced photocatalytic ability. The TiO_2 co-doped with N^{3-} and Ta^{5+} followed by loading with Fe_2O_3 excellently met the criteria for the persistent photocatalysts, which can be functional for environmental purification even after turning off lamp irradiation.

1. Introduction

For environmental purification, photocatalysis using semiconductors and sunlight has been attracting extensive attention [1–3]. The most extensively studied photocatalyst, TiO_2, possesses a wide band gap, such as 3.2 eV of anatase phase and 3.0 eV of rutile phase, and can absorb only the UV light occupying less than 5% of the total sunlight to generate charge carriers for promoting the surface redox reactions. In order to promote the practical application of TiO_2 the great challenge to overcome its inherent property is required.

To effectively harvest the visible light that occupies ~43% of the total sunlight [4], constructing a photocatalysis system with high visible-light activity is indispensable. Many efforts have been expended to modify the band gap of TiO_2 to absorb both UV and visible light. Among them, N doping has been most widely studied, and considered as the most promising visible light photocatalyst [5–8]. However, some researchers [6,9,10] also suggested the decrease in photocatalytic efficiency of N doped TiO_2, due to the strongly localized N 2p states at the top of the valence band, which would tend to trap photo-generated electrons, and also reduce the oxidation power and the mobility of holes. The anion vacancies caused by the N doping were also considered as a factor resulting in the decrease in photocatalytic efficiency.

As an approach to overcome these problems and to further enhance the photocatalytic activity of N doped TiO_2, the charge compensation by codoping with a transition metal ion has been proposed. The codoped TiO_2 with nonmetals and transition metals may be a new promising second-generation visible-light responsive photocatalyst, because the charge compensation by codoping may suppress the recombination of the photo-induced electrons and holes [11–15]. In this work, the facile microwave-assisted hydrothermal method was used for the synthesis of metal ion co-doped $TiO_{2-x}N_y$, while Ta^{5+} was selected as a codoped transition metal ion source. On the other hand, our previous work has reported that the $TiO_{2-x}N_y$ loaded with Fe_2O_3 showed excellent photocatalytic activity due to the heterogeneous electron transfer from $TiO_{2-x}N_y$ to Fe_2O_3 to retard the quick recombination of photo-generated electrons and holes [16]. To further enhance the photocatalytic activity of (Ta, N)-codoped TiO_2, a proper amount of Fe_2O_3 was loaded on the surface of samples via the microwave-assisted hydrothermal method.

Recently, we have prepared several fluorescence assisted photocatalysts including $TiO_{2-x}N_y$-based composite photocatalysts for the persistent photocatalytic degradation of NO in the dark after turning off light [17–20]. However, many investigations are still

* Corresponding author at: Institute of Multidisciplinary Research for Advanced Materials, Tohoku University, 2-1-1, Katahira, Aoba-ku, Sendai 980-8577, Japan. Tel.: +81 22 217 5598; fax: +81 22 217 5598.
** Corresponding author. Tel.: +81 22 217 5598; fax: +81 22 217 5598.
E-mail addresses: lihuihui@mail.tagen.tohoku.ac.jp, lihh@lzu.edu.cn (H. Li), shuyin@tagen.tohoku.ac.jp (S. Yin).

0926-3373/$ – see front matter © 2012 Elsevier B.V. All rights reserved.
http://dx.doi.org/10.1016/j.apcatb.2012.12.026

needed in this novel persistent fluorescence assisted photocatalytic system. First, although the codoping with Ta and N or the loading of Fe_2O_3 plays a role in the synthesis of visible light driven TiO_2 in published papers, the coupling of these two enhancements including the transfer of photogenerated carriers is not well demonstrated. Second, there is no direct evidence provided to prove the improved utilization of persistent fluorescence on such modified TiO_2, so it is necessary to illustrate a systematic and comprehensive mechanism and conduct corresponding experiments to support it. Herein, we further investigated the performances of the as-prepared (Ta, N)-codoped TiO_2/Fe_2O_3 after coupling with a long afterglow phosphor $CaAl_2O_4$:(Eu, Nd), especially the persistent fluorescence assisted photocatalytic activity. Our strategies can overcome the difficulties of some previous schemes and may provide some guidance for improving the photocatalytic activity of TiO_2 for practical application.

2. Experimental

The preparation method of Ta and N co-doped TiO_2 was similar to that of N doped TiO_2, which was reported in a previous paper [7]. After mixing 11.6 g of a 20 wt.% $TiCl_3$ aqueous solution with 10 cm^3 distilled water, the predetermined quantity (0.5 mol.% Ta) of $TaCl_5$ powders were dissolved into the solution, followed by the dissolution of 4.2 g of hexamethylenetetramine (HMT). The obtained solution was diverted into a Teflon® autoclave with an internal volume of 60 cm^3. The autoclave was irradiated by microwaves to start the hydrothermal reaction at the temperature of 190 °C for 10 min using a 1000 W microwave reaction apparatus (ACTAC Co. MWS-2, 2.45 GHz). After that, desired amounts of $FeCl_2{\cdot}4H_2O$ was added into the reaction solution, and the microwave assisted hydrothermal reaction was performed again at 190 °C for 10 min to get the products. The precipitates were separated by centrifugation, washed with distilled water and acetone three times, respectively, then vacuum dried at 60 °C overnight. The amount of Fe in the final products was changed in the range from 0 to 10 mol.%. The obtained TiO_2-based photocatalysts were then mixed with $CaAl_2O_4$:(Eu, Nd) micro-particles by a soft planetary ball milling with 200 rpm for 20 min, where the mass ratio of $CaAl_2O_4$:(Eu, Nd)/TiO_2 was adjusted to 3/2 [17–20].

The products were characterized by X-ray diffraction analysis (XRD, Shimadzu XD-D1), UV-vis spectrophotometry (Shimadzu, UV-2450), and BET specific surface area measurements (Quantachrome Instruments, NOVA 4200e). The chemical compositions were determined by the EDX spectrometer (Rayny EDX-800HS, Shimadzu) and CHN contents analysis (Yanaco, CHN Corder, MT-6). The low-level chemiluminescence intensity of singlet oxygen ($^1O_2$) was measured using a multiluminescence spectrometer (MLA-GOLDS; Tohoku Electric Ind., Japan) at 20 °C in the air. After placing approximately 1.2 g of the sample in a stainless steel sample chamber (50 mm in diameter), the blue light emitting diode (LED) light (wavelength 470 nm) was irradiated for 5 min. After that the chemiluminescence intensity corresponded to the singlet oxygen ($^1O_2$) at a wavelength of 643 nm was measured by subtracting the luminous intensity of $\lambda < 640$ nm from that of $\lambda < 620$ nm using two filters, $\lambda < 640$ nm and $\lambda < 620$ nm.

To evaluate the photocatalytic activities of the obtained samples, the oxidative decomposition of nitrogen monoxide and acetaldehyde were carried out.

The characterization system for the degradation of NO ($deNO_x$) used in the present research was similar to that of the Japanese Industrial Standard, which was established at the beginning of 2004 [21]. In this JIS standard, it is recommended that the photocatalytic activity of photocatalyst should be characterized by measuring the decrease in the concentration of NO at the outlet of a continuous flow reactor. One ppm of NO gas at a flow rate of 3.0 dm^3/min was introduced into a reactor, followed by irradiation by a lamp with the light wavelength of 300–400 nm.

The mechanism of photocatalytic $deNO_x$ had been researched carefully by M. Anpo. During the $deNO_x$ photocatalytic reaction, the nitrogen monoxide reacts with these reactive oxygen radicals, molecular oxygen, and very small amount of water in air to produce HNO_2 or HNO_3 [22]. It was confirmed that about 20% of nitrogen monoxide was decomposed to nitrogen and oxygen directly.

During the experiment, a 2 ppm standard NO gas (balance N_2) was mixed with air (1:1), and passing through the reactor (373 cm^3 of internal volume) continuously throughout the reaction. The flow rate of the reaction gas was 200 cm^3/min, and the gas retention time in the reactor was calculated as 112 s. The sample was placed in the hollow (20 mm × 16 mm × 0.5 mm) of a glass holder plate and set in the bottom center of the reactor. The light was turned on after having reached the adsorption equilibrium with flowing NO gas for more than 10 min. A 450 W high pressure mercury lamp was used as the light source, and different wavelengths were selected by several filters: Pyrex glass for > 290 nm, Kenko L41 Super Pro (W) filter > 400 nm and Fuji triacetyl cellulose filter (SC-50) > 510 nm. The concentration of NO was monitored using a NO_x analyzer (Yanaco, ECL-88A).

For the characterization of the persistent fluorescence assisted photocatalytic degradation of NO, experiment was proceeded as follows: Before light irradiation, the NO gas was continuously flowed through the reactor for 10 min to achieve diffusion and adsorption balance. Then, the light was irradiation for 30 min to realize the steady status of the photocatalytic degradation of NO and make long afterglow phosphor $CaAl_2O_4$:(Eu, Nd) absorb enough exciting energy. After that, the light was switched off, while the NO gas was flowed further for 3 h.

The photocatalytic activity for the acetaldehyde degradation was evaluated by measuring the changes in the concentrations of acetaldehyde and the decomposition product, CO_2. In order to obtain a homogeneous sample film for photocatalytic characterization, 0.3 g of sample powder was sufficiently mixed with 0.48 g xylene and 0.48 g 2-butanol, then dispersed on a glass substrate with an area of $\pi \times 25^2$ mm^2. The sample film was then heated at 140 °C for 30 min to evaporate the organic solvents. After irradiation by a 10 W black light for 1 h to eliminate the adsorbed organics on the surface, the sample film was placed in a sealed opaque reaction vessel (ca. 1.5 L), together with a desired amount of 10 mass% acetaldehyde (99%, Kanto Chem.) aqueous solution. The acetaldehyde was rapidly evaporated using an electric heater and fan, which were set in the inside of the reaction vessel. The persistent fluorescence assisted photocatalytic activity of the sample on degradation of acetaldehyde was evaluated as follows: after irradiating by a black light with the wavelength of 325 nm for 30 min, the sample was placed in the reaction vessel without irradiation, where the reaction was started by injecting and quickly evaporating 10 μL of acetaldehyde aqueous solution. About 5.0 mL of the gas was withdrawn from the reaction vessel through the injection hole every 30 min to determine the concentrations of the remaining acetaldehyde and generated CO_2 using a gas chromatograph (GC-2014 SHIMADZU).

As a preliminary experiment, the photocatalytic activity of the sample under photo-irradiation was also evaluated as follows: After keeping the sample in the dark for at least 40 min to realize the adsorption–desorption equilibrium, 40 μL of an acetaldehyde aqueous solution was injected and a simulated solar light (HAL-302, Ashahi) was irradiated to start the photocatalytic reaction. The average light intensity irradiated on the sample surface was about 69.3 W/m^2. The results are shown in the supporting information.

3. Resutls and discussion

The diffuse reflectance spectra of (Ta, N)-codoped TiO_2/Fe_2O_3, (Ta, N)-codoped TiO_2, N-doped TiO_2 and undoped TiO_2 (AEROXIDE® TiO_2 P25) are shown in Fig. 1. It can be seen that P25 absorbs only UV light because of the large band gap energy of ca. 3 eV, but (Ta, N)-codoped TiO_2/Fe_2O_3, (Ta, N)-codoped TiO_2 and N-doped TiO_2 absorb visible light up to 650 nm of the wavelength due to the creation of the new valence band of N2p. The visible light absorption ability did not change very much by codoping Ta^{5+} with N^{3-}. The increase in the visible light absorption ability by coupling with Fe_2O_3 must be due to the light absorption by Fe_2O_3 possessing smaller band gap energy. In addition, the spectra of Fe_2O_3 loading (Ta, N)-codoped TiO_2 showed red shift drastically with an increase in the amount of Fe, and the spectrum became very similar to that of Fe_2O_3 [16], as shown in Fig. S1.

The XRD patterns of (Ta, N)-codoped TiO_2/Fe_2O_3, (Ta, N)-codoped TiO_2, and N-doped TiO_2 titania samples were shown in Fig. S2. The structure of nitrogen-doped TiO_2 was confirmed as single rutile phase according to the existence of the (1 1 0) peak at $2\theta = 27^\circ$. However, mixed crystalline phases of anatase and rutile were found for all the Ta contained titania. The results suggested that comparing with the affect of Fe ion, the codoping with Ta showed greater influence on the crystalline phases of the samples and was with benefit for the formation of anatase phase. The samples with mixed crystalline phases were also expected to show high photocatalytic activities, attributed to the effective charge separation, similar to that for the high activity of P25 TiO_2 [29,30].

The photocatalytic activities of the samples were first evaluated by the photo-decomposition of NO_x gas under irradiation lights with various wavelengths. For a reference, the evaluation was also performed on P25. The initial concentration of NO_x was about 1.0 ppm, and during the experiment, gas containing 1.0 ppm NO_x was passed through the reactor continuously. The experiment was started when the concentration of NO_x at the outlet of the reactor reaching a steady value near 1.0 ppm. Then the light was turned on to start the photocatalytic reaction, and after reaching the concentration of NO_x to a steady value, the filter was changed so as to evaluate the activity under the irradiation with another wavelength region.

As shown in Fig. 2A, P25 showed no activity under visible-light irradiation with the wavelength of longer than 510 nm due to the large band-gap energy. In contrast, N-doped TiO_2 showed a high

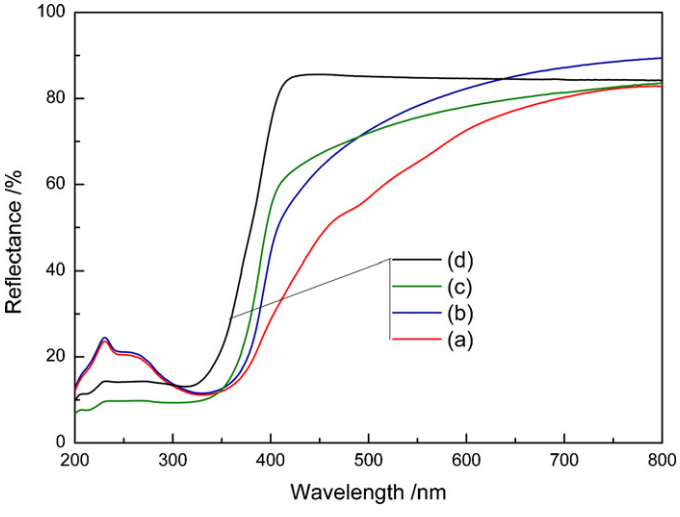

Fig. 1. Diffuse reflectance spectra of (a) (Ta, N)-codoped TiO_2/Fe_2O_3, (b) (Ta, N)-codoped TiO_2, (c) N-doped TiO_2 and (d) P25.

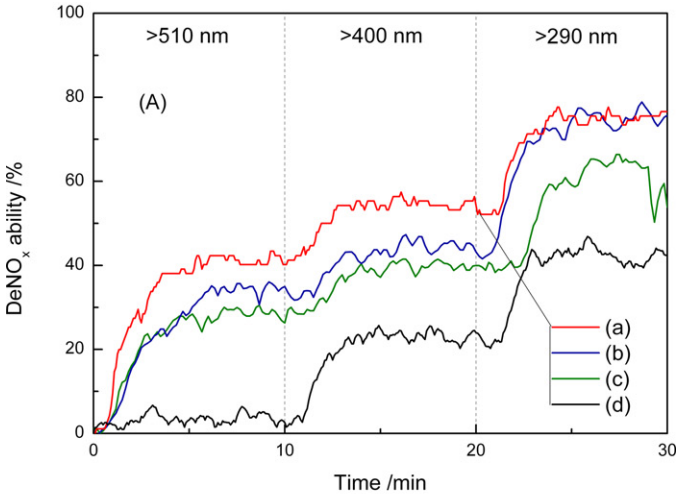

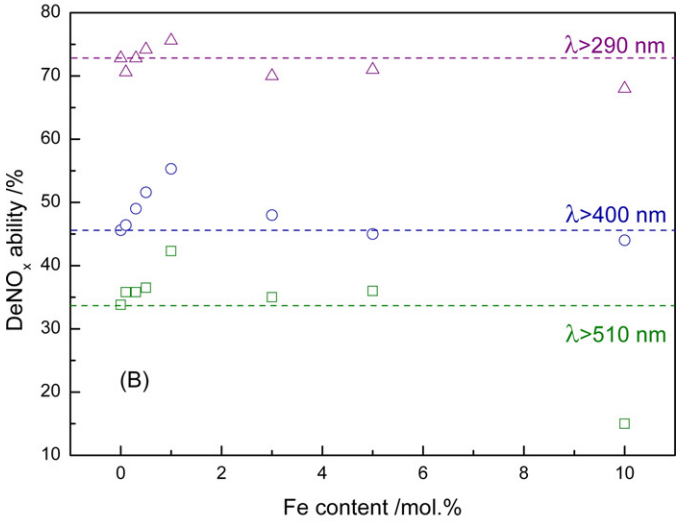

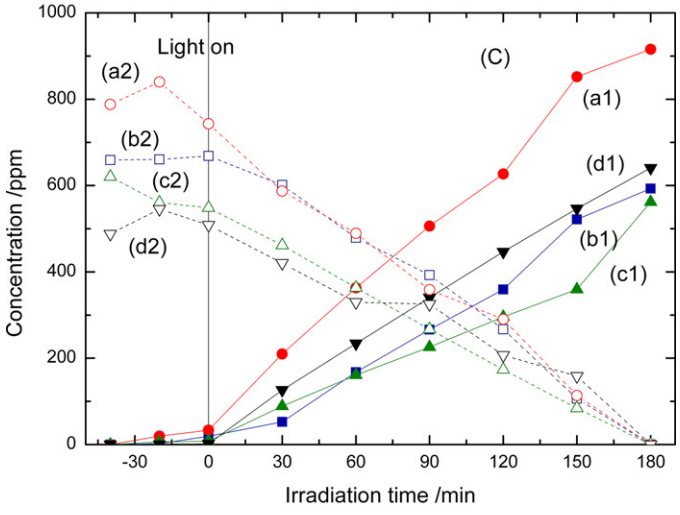

Fig. 2. (A) DeNO$_x$ ability of the composites consisted of (a) (Ta, N)-codoped TiO_2/Fe_2O_3, (b) (Ta, N)-codoped TiO_2, (c) N-doped TiO_2, (d) P25 under irradiation with different wavelengths, (B) photocatalytic activities for the oxidative decomposition of NO of (Ta, N)-codoped TiO_2/Fe_2O_3 with different Fe contents and (C) photocatalytic activities in decomposing acetaldehyde and generating carbon dioxide on (a) $CaAl_2O_4$:(Eu, Nd)/(Ta, N)-codoped TiO_2 coupled with Fe_2O_3, (b) $CaAl_2O_4$:(Eu, Nd)/(Ta, N)-codoped TiO_2, (c) $CaAl_2O_4$:(Eu, Nd)/N-doped TiO_2, (d) $CaAl_2O_4$:(Eu, Nd)/P25 under solar simulator irradiation with the intensity of 69.7 W/m^2 (1: CO_2 concentration, 2: CH_3CHO).

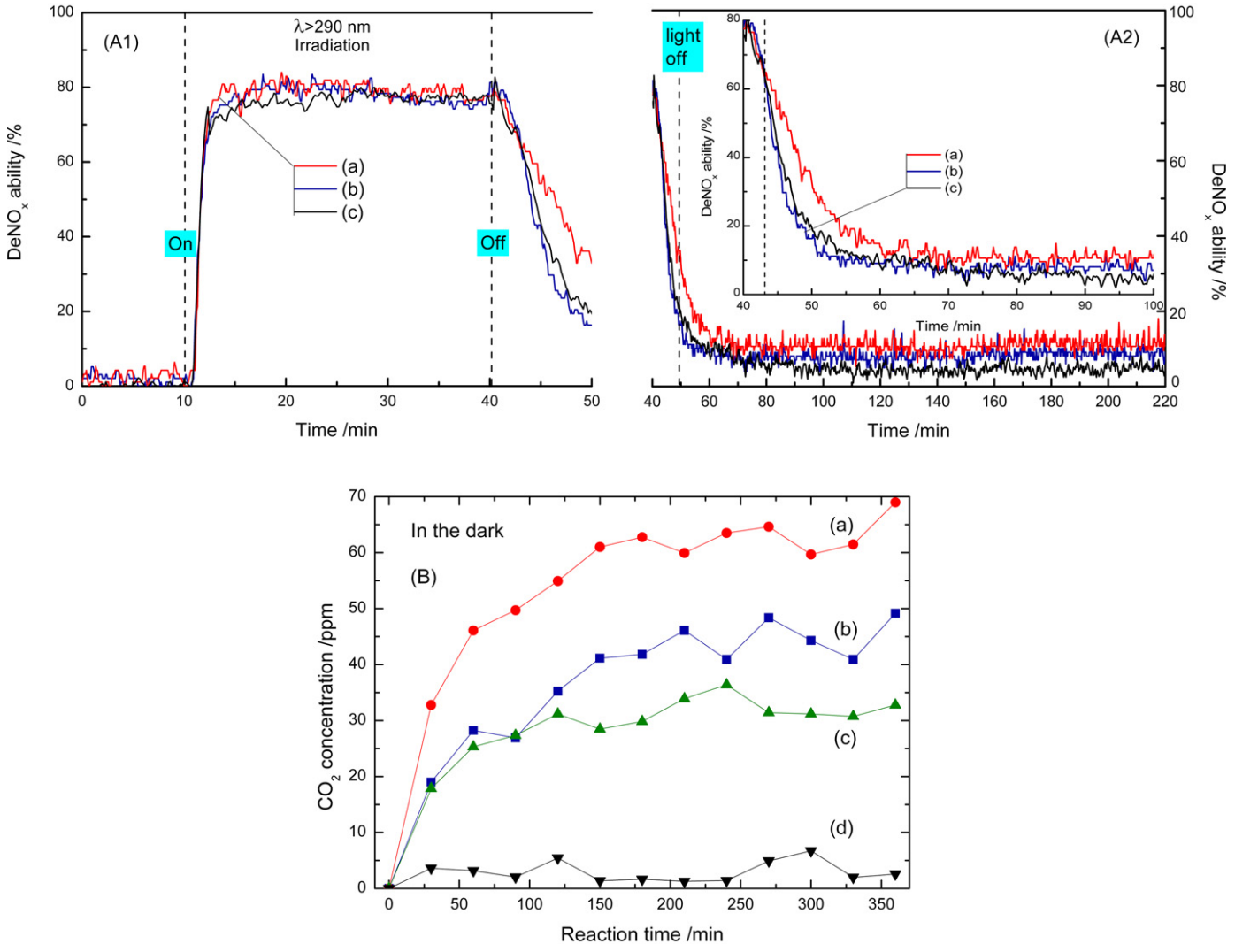

Fig. 3. (A) DeNO$_x$ ability of the composites of (a) (Ta, N)-codoped TiO_2/Fe_2O_3, (b) (Ta, N)-codoped TiO_2, (c) N-doped TiO_2, (d) P25 with $CaAl_2O_4$:(Eu, Nd) under (A1) a high pressure mercury arc irradiation with the wavelength of longer than 290 nm for 30 min followed by (A2) turning off light. The inset shows the result from 0 to 220 min. (B) Photocatalytic activities to generate carbon dioxide by decomposing acetaldehyde in the dark by (a) $CaAl_2O_4$:(Eu, Nd)/(Ta, N)-codoped TiO_2/Fe_2O_3, (b) $CaAl_2O_4$:(Eu, Nd)/(Ta, N)-codoped TiO_2, (c) $CaAl_2O_4$:(Eu, Nd)/N-doped TiO_2, (d) $CaAl_2O_4$:(Eu, Nd)/P25 irradiated by a black lamp for 30 min prior to start the reaction.

deNO$_x$ ability under both UV ($\lambda > 290$ nm) and visible ($\lambda > 400$ nm) light irradiation, higher than that of the commercial P25 TiO_2, due to the narrowed band gap and higher specific surface area [5–7]. To retard the quick recombination of photo-induced electrons and holes, co-doping of N^{3-} with Ta^{5+} ion has also been tried, where Ta^{5+} would occupy the Ti^{4+} sites to decrease the anion vacancy. By co-doping Ta^{5+} with N^{3-} into TiO_2, the photocatalytic efficiency of N-doped TiO_2 was effectively improved. In addition, after forming (Ta, N)-doped TiO_2/Fe_2O_3 composite, the activity was further enhanced, where the sample showed excellent photocatalytic activity especially under the visible light irradiation. This was attributable to the effective separation of photo-generated electrons and holes by the heterogeneous electron transfer from (Ta, N)-doped TiO_2 to Fe_2O_3.

The apparent quantum efficiencies of NO_x evolution were estimated on the basis of the number of incident photons, according to the photooxidation process of NO (Fig. S4 and Eq. (S1)) proposed by Yin et al. [23,24]. As shown in Fig. S5, the wavelength dependence of quantum efficiency is not consistent with the UV–vis spectrum. It is worthy to note that the quantum efficiency of modified TiO_2 at $\lambda > 510$ nm (~0.12%) was over 10 times higher than that of P25 (~0.015%), meantime the Brunauer–Emmett–Teller (BET) surface are of undoped TiO_2 P25 (80 $m^2\,g^{-1}$) was much smaller than that of modified TiO_2 (>200 $m^2\,g^{-1}$) (Fig. S3).

Because of the excellent visible light photocatalytic performance, (Ta, N)-codoped TiO_2 and (Ta, N)-codoped TiO_2/Fe_2O_3 were coupled with commercial long afterglow phosphor $CaAl_2O_4$:(Eu, Nd), which can emit persistent fluorescence ($\lambda_{ex} = 440$ nm) for more than 10 h to prepare the fluorescence assisted photocatalysts. The fluorescence ($\lambda_{ex} = 440$ nm) of $CaAl_2O_4$:(Eu, Nd) [17–20] belongs to the emission of $4f^65d^1 \rightarrow 4f^7$ electronic transition of Eu^{2+} ions in $CaAl_2O_4$ and seems to be used as a light source to excite (Ta, N)-codoped TiO_2 and $TiO_{2-x}N_y$ to proceed the photocatalytic reaction in the present systems. Fig. 3A shows the photocatalytic NO destruction behaviors of as-prepared samples after coupling with the same mass ratio of $CaAl_2O_4$:(Eu, Nd) under irradiation ($\lambda > 290$ nm) and after turning off the light. It was obvious that all the samples possessed similarly excellent photocatalytic deNO$_x$ activity under irradiation. Because a continuous reaction system was utilized in the present study, after turning off the light, usually it took about 10 min to return to the initial value of NO concentration. In our previous work, it was suggested that the degree of NO removal by P25-based composite and pure $TiO_{2-x}N_y$ immediately decreased after turning off the light [17–20].

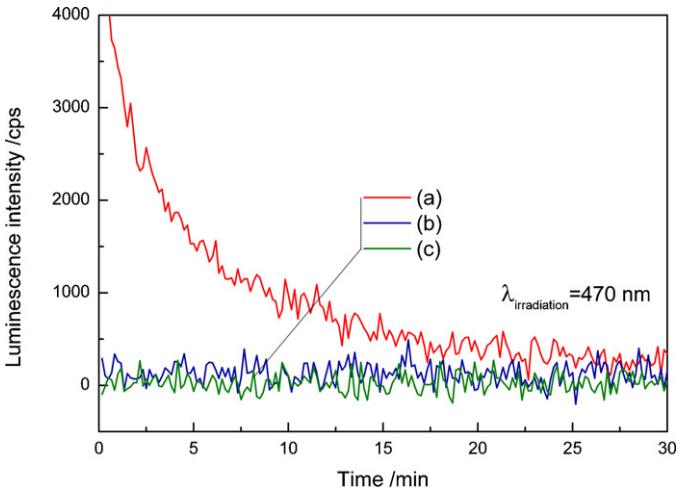

Fig. 4. Chemiluminescence emission spectra of $^1O_2$ generated at 25 °C in air under irradiation by blue LED light sources with the wavelength of 470 nm: (a) (Ta, N)-codoped TiO_2/Fe_2O_3, (b) (Ta, N)-codoped TiO_2, (c) N-doped TiO_2. (For interpretation of the references to color in figure legend, the reader is referred to the web version of the article.)

In contrast, $TiO_{2-x}N_y$, (Ta, N)-doped TiO_2 and (Ta, N)-doped TiO_2/Fe_2O_3 based-composites retained the NO destruction ability for about 3 h. The rutile phase $TiO_{2-x}N_y$ coupled with $CaAl_2O_4$:(Eu, Nd) showed the persistent photocatalytic deNO_x ability of only 4.2%, but (Ta, N)-codoped TiO_2 based-composite could continuously decompose 8.2% of NO_x. Moreover, (Ta, N)-codoped TiO_2 loaded with Fe_2O_3 showed the more excellent persistent deNO_x ability of 10.7%. The higher ability to generate $^1O_2$ of (Ta, N)-doped TiO_2/Fe_2O_3 shown in Fig. 4 might play an important role in inducing higher NO destruction ability after turning off the light than those of the others.

Above results show that the (Ta, N)-codoped TiO_2 is powerful for photocatalytic degradation of NO under both visible light and persistent fluorescence, and (Ta, N)-codoped TiO_2/Fe_2O_3 loaded with 1.0 mol.% of Fe_2O_3 exhibits the best performance (Fig. 2B). The strong ability to generate $^1O_2$ suggests the possibility of photocatalytic decomposition of some organic compounds under fluorescence irradiation with low intensity and/or solar light irradiation, as shown in Fig. 4. Here, we report that acetaldehyde (CH_3CHO), a common indoor air pollutant, can be efficiently decomposed over the composite samples both under solar light irradiation and after turning off the lamp irradiation.

Photocatalytic decomposition of CH_3CHO was investigated using a cylindrical static reaction vessel. As shown in Fig. 2C, all composites of $CaAl_2O_4$:(Eu, Nd)/P25, $CaAl_2O_4$:(Eu, Nd)/$TiO_{2-x}N_y$, $CaAl_2O_4$:(Eu, Nd)/(Ta, N)-codoped TiO_2 and $CaAl_2O_4$:(Eu, Nd)/(Ta, N)-codoped TiO_2/Fe_2O_3 showed the excellent acetaldehyde decomposition ability under photo irradiation (solar simulator), indicating the yield of carbon dioxide for 3 h of 62.8, 50.4, 50.5 and 59.4%, respectively. However, similar to NO removal, the persistent fluorescence assisted photocatalytic performances of the composites for decomposition of CH_3CHO to CO_2 in the dark greatly changed depending on the composition. The time dependences of the concentrations of carbon dioxide produced from the degradation of CH_3CHO with various samples are shown in Fig. 3B. All the composites were irradiated by black lamp for 30 min to get enough energy to generate long afterglow fluorescence, and then placed in the reactor to start the acetaldehyde decomposition without photo irradiation. The blank experiment using $CaAl_2O_4$:(Eu, Nd)/P25 composite showed that there is no noticeable change in the concentration of CO_2 in the dark. It is an indirect proof

Table 1
Ta, N, Fe contents in the as-prepared samples.

Sample	Ta (mol.%)	N (mol.%)	Fe (mol.%)
$TiO_{2-x}N_y$	0	0.051	0
$TiO_{2-x}N_y$ + 0.5%Ta	0.64	0.054	0
$TiO_{2-x}N_y$ + 0.5%Ta + 1%Fe	0.61	0.054	1.1

that acetaldehyde is stable and cannot be decomposed without photo-excitation of a catalyst. It is obvious that the amount of carbon dioxide generated greatly varied in the order $CaAl_2O_4$:(Eu, Nd)/(Ta, N)-codoped TiO_2/Fe_2O_3 > $CaAl_2O_4$:(Eu, Nd)/(Ta, N)-codoped TiO_2 > $CaAl_2O_4$:(Eu, Nd)/$TiO_{2-x}N_y$ » $CaAl_2O_4$:(Eu, Nd)/P25. This result was in good agreement with that of above descrived NO destruction. To confirm the contents of Ta, N and Fe in the products, EDX and CHN analysis were carried out, and the results are summarized in Table 1. The detected Ta and Fe contents in the prepared samples mostly agreed well with the added values. About 0.054 mol.% N was detected in the N doped TiO_2. For the photocatalytic activities in the decomposition of CH_3CHO, the co-doping of Ta showed obvious positive effect in enhancing the activity, while the Fe_2O_3 loading caused the further increase in activity. The determining factor was attributed to the amount of anion vacancy, which could be reduced by a higher valence metal ion Ta co-doping, and the effective separation of photo-induced electrons and holes, which was increased by Fe_2O_3 loading.

Fig. 5 schematically shows the band structures of (Ta, N)-codoped TiO_2/Fe_2O_3. As a result of band gap energy (results shown in Fig. S6) calculated by UV–vis DRS spectrum (Fig. 1), it is confirmed that the hybridized states composed of N 2p orbitals and Ta 5d orbitals are formed after co-doping of N and Ta into TiO_2 [25–28]. The Fermi level lies above the hybridized states, and full occupied hybridized states appear in contrast to empty states caused by single doping. These fully occupied states in the valence band edge cannot act as recombination centers. Incorporation of Ta into N-doped TiO_2 changes the character of N 2p orbitals from isolated empty midgap states to fully occupied N 2p–Ta 5d hybridized states above the top of the valence band, while the Ta 5d state is located at the conduction band edge [28]. Moreover, the compensated systems of a continuum-like band keep the semiconductor character, which subsequently promotes the separation of electron–hole pairs excited under visible-light irradiation [26]. These results indicate that the compensated systems guarantee a significant photocatalytic activity in the visible-light region by narrowing the energy gap and suppress the recombination of electron–hole pairs. In addition, the coupling with Fe_2O_3 will result in the effective separation of photo-induced electrons and holes by the heterogeneous electron transfer from TiO_2 to Fe_2O_3.

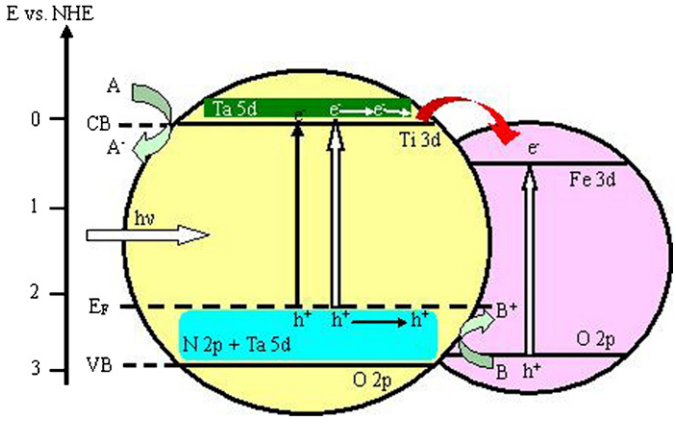

Fig. 5. Schematic illustration of the band structure of (Ta, N)-codoped TiO_2/Fe_2O_3.

4. Conclusions

A novel photocatalyst $CaAl_2O_4$:(Eu, Nd)/(Ta, N)-codoped TiO_2/Fe_2O_3, which shows the efficient decomposition ability of both NO and CH_3CHO under both light irradiation and persistent fluorescence irradiation was successfully developed. The enhanced photocatalytic activity of $CaAl_2O_4$:(Eu, Nd)/(Ta, N)-codoped TiO_2 is attributed to the modulated band structure formed by a hybrid conduction band of the empty (Ti 3d + Ta 5d) orbitals and a hybrid valence band of the occupied (O 2p + N 2p) orbitals. Furthermore, the photocatalytic activity of $CaAl_2O_4$:(Eu, Nd)/(Ta, N)-codoped TiO_2 could be greatly improved by coupling with Fe_2O_3, probably due to the depression of the recombination of photo-induced electrons and holes by the heterogeneous electron transfer. The present study proves that making solid-solution oxides is a feasible approach for developing highly visible-light-active semiconductor photocatalysts.

Acknowledgements

This research was supported in part by the Management Expenses Grants for National Universities Corporations from the Ministry of Education, Culture, Sports, Science for Technology of Japan (MEXT), and by the Grant-in-Aid for Science Research (No. 20360293 & No. 22651022). The authors acknowledge the assistance from the Hatano Foundation.

Appendix A. Supplementary data

Supplementary data associated with this article can be found, in the online version, at http://dx.doi.org/10.1016/j.apcatb.2012.12.026.

References

[1] M.R. Hoffmann, S.T. Martin, W. Choi, D.W. Bahnemann, Chemical Reviews 95 (1995) 69–96.
[2] A.L. Linsebigler, G.Q. Lu, J.T. Yates, Chemical Reviews 95 (1995) 735–758.
[3] A. Fujishima, K. Hashimoto, T. Watanabe, TiO_2 Photocatalysis: Fundamentals and Applications, BKC Inc., Tokyo, Japan, 1999, pp. 80–114.
[4] D. Wang, T. Kako, J. Ye, Journal of the American Chemical Society 130 (2008) 2724–2725.
[5] R. Asahi, T. Morikawa, T. Ohwaki, K. Aoki, Y. Taga, Science 293 (2001) 269–271.
[6] H. Irie, Y. Watanabe, K. Hashimoto, Journal of Physical Chemistry B 107 (2003) 5483–5486.
[7] S. Yin, H. Yamaki, M. Komatsu, Q. Zhang, J. Wang, Q. Tang, F. Saito, T. Sato, Journal of Materials Chemistry 13 (2003) 2996–3001.
[8] J. Wang, S. Yin, Q. Zhang, F. Saito, T. Sato, Journal of Materials Chemistry 13 (2003) 2348–2352.
[9] C. Burda, Y. Lou, X. Chen, A.C.S. Samia, J. Stout, J.M. Gole, Nano Letters 3 (2003) 1049–1051.
[10] S. Sakthivel, M. Janczarek, H. Kisch, Journal of Physical Chemistry B 108 (2004) 19384–19387.
[11] Y.Q. Gai, J.B. Li, S.S. Li, J.B. Xia, S.H. Wei, Physical Review Letters 102 (2009) 036402–036405.
[12] Z.Y. Zhao, Q.J. Liu, Catalysis Letters 124 (2008) 111–117.
[13] W.J. Yin, H.W. Tang, S.H. Wei, M.M. Al-Jassim, J. Turner, Y.F. Yan, Physical Review B 82 (2010) 045106(1)–045106(6).
[14] D.E. Gu, B.C. Yang, Y.D. Hu, Catalysis Communications 9 (2008) 1472–1476.
[15] J.W. Liu, R. Han, Y. Zhao, H.T. Wang, W.J. Lu, T.F. Yu, Y.X. Zhang, Journal of Physical Chemistry C 115 (2011) 4507–4515.
[16] P. Zhang, S. Yin, T. Sato, Applied Catalysis B 103 (2011) 462–469.
[17] H.H. Li, S. Yin, T. Sato, Nanoscale Research Letters 6 (2011) 5–8.
[18] H.H. Li, S. Yin, T. Sato, Applied Catalysis B 106 (2011) 586–591.
[19] H.H. Li, S. Yin, Y. Wang, T. Sato, Journal of Catalysis 286 (2012) 273–278.
[20] (a) H.H. Li, S. Yin, Y. Wang, T. Sato, RSC Advances 2 (2012) 3234–3236; (b) H.H. Li, S. Yin, Y. Wang, T. Sato, Environmental Science and Technology 46 (2012) 7741–7745.
[21] Japanese Industrial Standard (JIS R 1701-1:2004(J)), Test method for air purification performance of photocatalytic materials – Part 1: removal of nitric oxide, Japanese Standards Association, Established on 2004-01-20.
[22] M. Anpo, Recent Development on Visible Light Response Type Photocatalyst, NTS, Tokyo, 2002, ISBN 4-86043-009-03, p. 9.
[23] S. Yin, K. Ihara, Y. Aita, M. Komatsu, T. Sato, Journal of Photochemistry and Photobiology A 179 (2006) 105–114.
[24] S. Yin, B. Liu, P. Zhang, T. Morikawa, K. Yamanaka, T. Sato, Journal of Physical Chemistry C 112 (2008) 12425–12431.
[25] J. Tang, J. Ye, Chemical Physics Letters 410 (2005) 104–107.
[26] X. Ma, Y. Wu, Y. Lu, J. Xu, Y. Wang, Y. Zhu, Journal of Physical Chemistry C 115 (2011) 16963–16969.
[27] P. Zhang, S. Yin, T. Sato, Advances in Science and Technology 63 (2010) 36–40.
[28] R. Long, N.J. English, Chemical Physics Letters 478 (2009) 175–179.
[29] D. Hurum, A. Agrios, K. Gray, Journal of Physical Chemistry B 107 (2003) 4545–4549.
[30] T. Ohno, K. Tokieda, S. Higashida, M. Matsumura, Applied Catalysis A 244 (2003) 383–391.